Inorganic Chemistry
Article

Inorg. Chem. **2009**, *48*, 10249–10256 **10249**
DOI: 10.1021/ic9012685

Full- or Half-Encapsulation of Sulfate Anion by a Tris(3-pyridylurea) Receptor: Effect of the Secondary Coordination Sphere†

Fuyu Zhuge,[‡,⊥] Biao Wu,[*,‡,§] Jianjun Liang,[‡] Jin Yang,[§] Yanyan Liu,[‡,⊥] Chuandong Jia,[‡,⊥] Christoph Janiak,[*,∥] Ning Tang,[§] and Xiao-Juan Yang[*,‡,§]

[‡]*State Key Laboratory for Oxo Synthesis & Selective Oxidation, Lanzhou Institute of Chemical Physics, Chinese Academy of Sciences, Lanzhou 730000, China,* [§]*State Key Laboratory of Applied Organic Chemistry, Lanzhou University, Lanzhou 730000, China,* [⊥]*Graduate School of Chinese Academy of Sciences, Beijing 100049, China, and* [∥]*Institut für Anorganische und Analytische Chemie, Universität Freiburg, Albertstrasse 21, D-79104 Freiburg, Germany*

Received July 2, 2009

Self-assembly of the $[Fe(DABP)_3]SO_4$ (DABP = 5,5′-diamino-2,2′-bipyridine) or $[Fe(bipy)_3]SO_4$ (bipy = 2,2′-bipyridine) complex with a tripodal tris(3-pyridylurea) ligand (L) results in a layered structure that includes a sulfate anion in the cleft of *one* L molecule. The two compounds, $[Fe(DABP)_3][SO_4{\subset}L]\cdot 10H_2O$ (**2**) and $[Fe(bipy)_3][SO_4{\subset}L]\cdot 9H_2O$ (**3**), show very similar sheets formed by the anionic units $[SO_4{\subset}L]^{2-}$ and cationic building blocks ($[Fe(DABP)_3]^{2+}$ or $[Fe(bipy)_3]^{2+}$). However, there are different water clusters that link the adjacent layers in the two products, that is, water parallelograms and quasi "water cubes" in **2** versus single water molecules, water dimers, and hexamers in **3**. The half-encapsulation of sulfate by a single L molecule contrasts with the previously reported full-encapsulation of the sulfate ion by two L molecules in $[M(H_2O)_6][SO_4{\subset}L_2]$ (**1**). This different anion encapsulation is traced to the hydrogen-acceptor properties of the pyridyl groups of L together with the hydrogen-bonding properties of the cation secondary coordination sphere for a solid-state packing optimization. In **1** the direct hydrogen bonding from the secondary coordination sphere of octahedral $[M(H_2O)_6]^{2+}$ to L-pyridyl helps in the formation of an octahedral cation−anion coordination in the NaCl-type structure. In **2** and **3**, crystal water instead of the cations has to satisfy the hydrogen-accepting demands of L. Consequently, a non-spherical and only partly water-surrounded half-encapsulated $[SO_4{\subset}L]^{2-}$ anion allows for a closer approach of the $[Fe(DABP)_3]^{2+}$ or $[Fe(bipy)_3]^{2+}$ cations than the $[SO_4{\subset}L_2]^{2-}$ anion. Then, the similar cation and anion size in **2** and **3** with the Coulomb attraction confined to a two-dimensional plane leads to the formation of a hexagonal BN (or graphite) lattice. Competition experiments with different anions for compound **2** reveal that SO_4^{2-} can be selectively crystallized against NO_3^-, OAc^-, or ClO_4^-.

Introduction

Anions play numerous indispensable roles in biology, medicine, catalysis, environmental events, and so forth, and the coordination chemistry of anions has become an important aspect in supramolecular chemistry.[1,2] A large number of synthetic anion receptors have been designed by incorporating hydrogen bonding donors such as NH moieties.[3] Urea and thiourea functionalities are promising hydrogen bonding donors because the two NH groups can form chelating hydrogen bonds with oxoanions, and (oligo)urea derivatives represent a class of excellent anion receptors by taking

† Dedicated to Prof. Xin-Tao Wu on the occasion of his 70th birthday.

*To whom correspondence should be addressed. E-mail: wubiao@lzb.ac.cn (B.W.), janiak@uni-freiburg.de (C.J.), yangxj@lzb.ac.cn (X.-J.Y.).

(1) (a) Special issue, *Coord. Chem. Rev.* **2003**, *240* (1−2). (b) Beer, P. D.; Gale, P. A. *Angew. Chem., Int. Ed.* **2001**, *40*, 486–516. (c) Caltagirone, C.; Gale, P. A. *Chem. Soc. Rev.* **2009**, *38*, 520–563. (d) Gale, P. A.; García-Garrido, S. E.; Garric, J. *Chem. Soc. Rev.* **2008**, *37*, 151–190. (e) Steed, J. W. *Chem. Soc. Rev.* **2009**, *38*, 506–519.

(2) (a) Bowman-James, K. *Acc. Chem. Res.* **2005**, *38*, 671–678. (b) Amendola, V.; Esteban-Gómez, D.; Fabbrizzi, L.; Licchelli, M. *Acc. Chem. Res.* **2006**, *39*, 343–353. (c) Wichmann, K.; Antonioli, B.; Söhnel, T.; Wenzel, M.; Gloe, K.; Price, J. R.; Lindoy, L. F.; Blake, A. J.; Schröder, M. *Coord. Chem. Rev.* **2006**, *250*, 2987–3003. (d) Pérez, J.; Riera, L.; Ion, L.; Riera, V.; Anderson, K. M.; Steed, J. W.; Miguel, D. *Dalton Trans.* **2008**, 878–886.

(3) (a) McKee, V.; Nelson, J.; Town, R. M. *Chem. Soc. Rev.* **2003**, *32*, 309–325. (b) Katayev, E. A.; Pantos, C. D.; Reshetova, M. D.; Khrustalev, V. N.; Lynch, V. M.; Ustynyuk, J. A.; Sessler, J. L. *Angew. Chem., Int. Ed.* **2005**, *44*, 7386–7390. (c) Kang, S. O.; Hossain, M. A.; Powell, D.; Bowman-James, K. *Chem. Commun.* **2005**, 328–330. (d) Nelson, J.; Nieuwenhuyzen, M.; Pál, I.; Town, R. M. *Dalton Trans.* **2004**, 2303–2308. (e) Seidel, D.; Lynch, V.; Sessler, J. L. *Angew. Chem., Int. Ed.* **2002**, *41*, 1422–1425. (f) Ju, J.; Park, M.; Suk, J.-m.; Lah, M. S.; Jeong, K.-S. *Chem. Commun.* **2008**, 3546–3548.

(4) (a) Custelcean, R. *Chem. Commun.* **2008**, 295–307. (b) Caltagirone, C.; Hiscock, J. R.; Hursthouse, M. B.; Light, M. E.; Gale, P. A. *Chem.−Eur. J.* **2008**, *14*, 10236–10243. (c) Caltagirone, C.; Gale, P. A.; Hiscock, J. R.; Brooks, S. J.; Hursthouse, M. B.; Light, M. E. *Chem. Commun.* **2008**, 3007–3009. (d) Fisher, M. G.; Gale, P. A.; Light, M. E.; Loeb, S. J. *Chem. Commun.* **2008**, 5695–5697. (e) Bondy, C. R.; Gale, P. A.; Loeb, S. J. *J. Am. Chem. Soc.* **2004**, *126*, 5030–5031. (f) Meshcheryakov, D.; Arnaud-Neu, F.; Bohmer, V.; Bolte, M.; Cavaleri, J.; Hubscher-Bruder, V.; Thondorf, I.; Werner, S. *Org. Biomol. Chem.* **2008**, *6*, 3244–3225. (g) Li, X.; Li, H.; Yu, S.-Y.; Li, Y.-Z. *Sci. China Ser. B-Chem.* **2009**, *52*, 471–474.

Published on Web 09/29/2009

advantage of their cooperative multiple binding sites and shape complementarities.[4,5] The binding and separation of sulfate ions from aqueous phases by synthetic receptors is of interest yet challenging to chemists because of the high charge density and hydration energy of this anion.[6] A few tripodal receptors have been shown to be able to encapsulate SO_4^{2-} ion effectively by multiple hydrogen bonds from their hydrogen-bonding donors.[7a,8]

Recently we have designed a series of oligourea anion receptors,[7] including a tren-based tris(3-pyridylurea) compound (L) which can encapsulate a sulfate anion in the cavity formed by two L molecules in the hydrogen-bonded architecture $[M(H_2O)_6][SO_4\subset L_2]$ (M = Mn, Zn) (**1a**, **1b**) from the reaction of MSO_4 with L.[7a] The same results have also been reported by Custelcean et al.[8c,e] It is noticed that in **1** the pyridyl ends of the tripodal ligand L do not coordinate directly to the metal ion, but interact with the hydrated metal cation $[M(H_2O)_6]^{2+}$ through hydrogen bonding between the nitrogen atoms and the coordinated water molecules ($O-H\cdots N_{py}$). These results imply that the sulfate capsules found in **1** may also be generated via the second-sphere coordination by using other complexes containing hydrogen-bond donors. Therefore, we chose the $[Fe(DABP)_3]SO_4$ (DABP = 5,5′-diamino-2,2′-bipyridine) complex, which has been proven to be able to serve as a building block in the construction of large supramolecular architectures via hydrogen bonding interactions of the free amino groups,[9,10] to assemble with the ligand L. Herein we report the formation of sulfate-included networks with the compositions $[Fe(DABP)_3][SO_4\subset L]\cdot 10H_2O$ (**2**) and $[Fe(bipy)_3][SO_4\subset L]\cdot 9H_2O$ (**3**), both with a half-encapsulated $[SO_4\subset L]^{2-}$ anion (Scheme 1). Furthermore, full- versus half anion encapsulation is traced to the metal-cation second-sphere coordination in connection with solid-state packing arguments.

Experimental Section

General Procedures. ^{1}H NMR spectra were recorded on a Bruker AV400 instrument with calibration against the solvent signal (DMSO-d_6, 2.50 ppm for ^{1}H). IR spectra were measured using a Nicolet AVATAR 360 FT-IR spectrometer as KBr disks. Elemental analyses were performed on a VarioEL from Elementaranalysensysteme GmbH. ESI-MS measurements were carried out using a Waters ZQ4000 spectrometer in methanol/water. Melting points were detected on an X-4 Digital Vision MP instrument. Powder X-ray diffraction patterns were obtained with a D/max RB diffractometer using Cu Kα radiation. Thermogravimetry was carried out under N_2 flow (60 mL min^{-1}) with a Pyris Diamond TG/DAT instrument at a heating rate of 10 °C min^{-1} up to 1000 °C.

Scheme 1. Schematic Representation of the 1:1 and 1:2 Sulfate Encapsulation in Compounds **1**−**3**

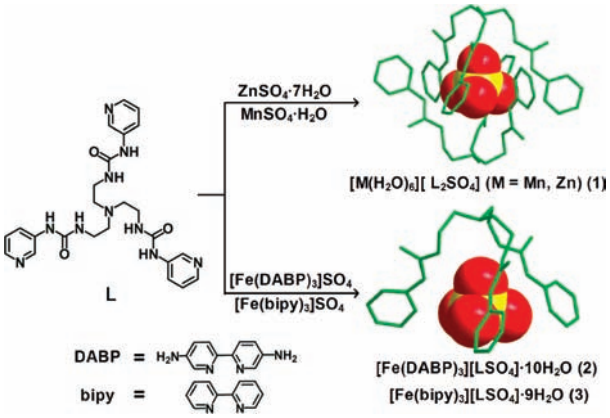

Scheme 2. Numbering Scheme for DABP and bipy

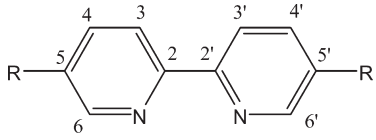

Synthesis of $[Fe(DABP)_3][SO_4\subset L]\cdot 10H_2O$ (2). The ligand *N*-[2-[bis[2-[*N*′-(3-pyridyl)ureido]ethyl]-amino]ethyl]-*N*′-(3-pyridyl)-urea (L), 5,5′-diamino-2,2′-bipyridine (DABP, Scheme 2) and its iron(II) complex, $[Fe(DABP)_3]SO_4$, were prepared following previously published procedures.[7a,9] An aqueous solution (10 mL) of the in situ prepared $[Fe(DABP)_3]SO_4$ (0.05 mmol) was combined with a methanol solution (10 mL) of L (25 mg, 0.05 mmol). The solvent was then allowed to evaporate slowly at room temperature. After 1 week, red crystals of compound **2** were obtained. Yield: 52 mg (75%). Mp > 300 °C. Positive-ion mode ESI-MS: *m*/*z* 187.3 ($[DABP + H]^+$), 214.3 ($[Fe(DABP)_2]^{2+}$), 307.5 ($[Fe(DABP)_3]^{2+}$), 467.6 ($[Fe(DABP)_2 + L]^{2+}$), 507.6 ($[L + H]^+$), 560.6 ($[Fe(DABP)_3 + L]^{2+}$); Negative-ion mode ESI-MS: 301.0 ($[L + SO_4]^{2-}$), 505.2 ($[L - H]^-$), 554.3 ($[2\ L + SO_4]^{2-}$), 603.1 ($[L + HSO_4]^-$). Anal. Found: C, 47.04; H, 5.39; N, 22.85. Calcd. for $[Fe(DABP)_3][SO_4\subset L]\cdot 9H_2O$ ($C_{54}H_{78}FeN_{22}O_{16}S$): C, 47.04; H, 5.70; N, 22.34%. ^{1}H NMR (DMSO-d_6, 400 MHz): 2.36 (s, 6H, $N-CH_2-$), 3.07 (s, 6H, urea$-CH_2-$), 5.93 (s, 12H, NH_2), 6.57 (d, J = 1.9 Hz, 6H, DABP-H6, H6′), 7.06 (m, 9H, Py-H5, DABP-H4, H4′), 7.93 (m, 6H, Py-H4, H6), 8.0 (d, J = 8.8 Hz, 6H, DABP-H3, H3′), 8.22 (s, 3H, NH), 8.77 (s, 3H, Py-H2), 10.22 (s, 3H, NH). FT-IR (KBr, ν/cm^{-1}): 3339 m (br.), 3222 m (br.), 3048 m, 2813 w, 1669 s (br.) (C═O), 1601 s, 1577 s, 1550 s (br.), 1485 s, 1420 m, 1296 m, 1263 m, 1230 m, 1190 w, 1111 m (br.), 1066 m, 1027 w, 973 w, 881 w, 843 w, 802 w, 706 w, 609 w, 560 w, 543 w, 448 w, 405 w.

Synthesis of $[Fe(bipy)_3][SO_4\subset L]\cdot 9H_2O$ (3). The preparation of $[Fe(bipy)_3]SO_4$ was similar to that of $[Fe(DABP)_3]SO_4$ except that DABP was replaced by bipy (bipy = 2,2′-bipyridine, Scheme 2). An aqueous solution (10 mL) containing $FeSO_4\cdot 7H_2O$ (14 mg, 0.05 mmol) and bipy (23 mg, 0.15 mmol) was heated and then

(5) (a) Allevi, M.; Bonizzoni, M.; Fabbrizzi, L. *Chem.*−*Eur. J.* **2007**, *13*, 3787–3795. (b) Turner, D. R.; Paterson, M. J.; Steed, J. W. *J. Org. Chem.* **2006**, *71*, 1598–1608. (c) Lakshminarayanan, P. S.; Ravikumar, I.; Suresh, E.; Ghosh, P. *Chem. Commun.* **2007**, 5214–5216. (d) Ravikumar, I.; Lakshminarayanan, P. S.; Arunachalam, M.; Suresh, E.; Ghosh, P. *Dalton Trans.* **2009**, 4160–4168.

(6) (a) Mullen, K. M.; Beer, P. D. *Chem. Soc. Rev.* **2009**, *38*, 1701–1713. (b) Moyer, B. A.; Bonnesen, P. V. Physical Factors in Anion Separations. In *Supramolecular Chemistry of Anions*; Bianchi, A., Bowman-James, K., García-España, E., Eds.; Wiley-VCH: New York, 1997.

(7) (a) Wu, B.; Liang, J.; Yang, J.; Jia, C.; Yang, X.-J.; Zhang, H.; Tang, N.; Janiak, C. *Chem. Commun.* **2008**, 1762–1764. (b) Wu, B.; Huang, X.; Xia, Y.; Yang, X.-J.; Janiak, C. *CrystEngComm* **2007**, *9*, 676–685. (c) Wu, B.; Huang, X.; Liang, J.; Liu, Y.; Yang, X.-J.; Hu, H.-M. *Inorg. Chem. Commun.* **2007**, *10*, 563–566. (d) Liang, J.; Wu, B.; Jia, C.; Yang, X.-J. *CrystEngComm* **2009**, *11*, 975–977.

(8) (a) Jose, D. A.; Kumar, D. K.; Ganguly, B.; Das, A. *Inorg. Chem.* **2007**, *46*, 5817–5819. (b) Raposo, C.; Almaraz, M.; Martín, M.; Weinrich, V.; Mussóns, M. L.; Alcázar, V.; Caballero, M. C.; Morán, J. R. *Chem. Lett.* **1995**, 759–760. (c) Custelcean, R.; Remy, P.; Bonnesen, P. V.; Jiang, D.-e.; Moyer, B. A. *Angew. Chem., Int. Ed.* **2008**, *47*, 1866–1870. (d) Custelcean, R.; Moyer, B. A.; Hay, B. P. *Chem. Commun.* **2005**, 5971–5973. (e) Custelcean, R.; Remy, P. *Cryst. Growth Des.* **2009**, *9*, 1985–1989.

(9) Janiak, C.; Deblon, S.; Wu, H.-P.; Kolm, M. J.; Klüfers, P.; Piotrowski, H.; Mayer, P. *Eur. J. Inorg. Chem.* **1999**, 1507–1521.

(10) (a) Wu, B.; Yang, X.-J.; Janiak, C.; Lassahn, P. G. *Chem. Commun.* **2003**, 902–903. (b) Yang, X.-J.; Wu, B.; Janiak, C. *CrystEngComm* **2004**, *6*, 126–129. (c) Yang, X.-J.; Wu, B.; Janiak, C.; Sun, W.-H.; Hu, H.-M. *Z. Anorg. Allg. Chem.* **2004**, *630*, 1564–1572. (d) Yang, X.-J.; Wu, B.; Sun, W.-H.; Janiak, C. *Inorg. Chim. Acta* **2003**, *343*, 366–372. (e) Yang, X.-J.; Janiak, C.; Heinze, J.; Drepper, F.; Mayer, P.; Piotrowski, H.; Klüfers, P. *Inorg. Chim. Acta* **2001**, *318*, 103–116.

combined with a methanol solution (10 mL) of L (25 mg, 0.05 mmol). The reaction mixture was heated and then filtered. Red crystals were obtained either by slow diffusion of diethyl ether into the filtrate or by slow evaporation of the filtrate in the presence of diethyl ether solvent at room temperature for several days. Yield: 41 mg (70%). Mp > 300 °C. Positive-ion mode ESI-MS: *m*/*z* 157.3 ($[bipy + H]^+$), 184.3 ($[Fe(bipy)_2]^{2+}$), 262.4 ($[Fe(bipy)_3]^{2+}$), 507.6 ($[L + H]^+$); Negative-ion mode ESI-MS: 301.0 ($[L + SO_4]^{2-}$), 505.2 ($[L - H]^-$), 554.3 ($[2\,L + SO_4]^{2-}$), 603.3 ($[L + HSO_4]^-$). Anal. Found: C, 51.10; H, 4.91; N, 17.95. Calcd. For $[Fe(bipy)_3][SO_4{\subset}L]\cdot 7.5H_2O$ ($C_{54}H_{69}FeN_{16}O_{14.5}S$): C, 51.39; H, 5.51; N, 17.76%. ^{1}H NMR (DMSO-d_6, 400 MHz), 2.42 (s, 6H, N−CH_2−), 3.09 (s, 6H, urea−CH_2−), 7.04 (s, 3H, NH), 7.37 (d, J = 5.3 Hz, 3H, Py-H5), 7.46 (dd, J = 5.1, 6.9 Hz, 2H, bipy-H5, H5′), 7.52 (t, J = 6.0 Hz, 4H, bipy-H5, H5′), 7.64 (s, 3H, Py-H4), 7.86 (d, 3H, Py-H6), 7.94 (s, 6H, bipy-H4, H4′), 8.21 (s, 4H, bipy-H3, H3′), 8.39 (d, 2H, bipy-H3, H3′), 8.69 (d, 6H, bipy-H6, H6′), 8.86 (d, 3H, Py-H2), 9.73 (s, 3H, NH). FT-IR (KBr, ν/cm−1): 3251 s (br.), 3109 m, 3048 m (br.), 2815 w, 1684 s (C═O), 1602 m, 1546 s, 1483 s, 1443 m, 1424 m, 1354 w, 1294 m, 1259 m, 1226 m, 1189 w, 1117 s (br.), 1067 m, 933 w, 834 w, 803 m, 777 m, 732 m, 710 m, 616 m, 554 w, 499 w, 443 w, 409 w.

Competitive Crystallization Experiment of 2. DABP (28 mg, 0.15 mmol) was added to an aqueous solution (10 mL) containing $FeSO_4\cdot 7H_2O$ (14 mg, 0.05 mmol), $NaOAc\cdot 3H_2O$ (7 mg, 0.05 mmol), $NaNO_3$ (4 mg, 0.05 mmol), and $NaClO_4$ (6 mg, 0.05 mmol). The mixture was heated for 10 min, and a methanol solution (10 mL) of L (25 mg, 0.05 mmol) was added. The solvent was allowed to evaporate slowly at room temperature. After 1 week, red crystals were obtained. Mp > 300 °C. Positive-ion mode ESI-MS: *m*/*z* 187.3 ($[DABP + H]^+$), 214.3 ($[Fe(DABP)_2]^{2+}$), 307.5 ($[Fe(DABP)_3]^{2+}$), 467.6 ($[Fe(DABP)_2 + L]^{2+}$), 507.7 ($[L + H]^+$), 560.7 ($[Fe(DABP)_3 + L]^{2+}$); Negative-ion mode ESI-MS: 301.0 ($[L + SO_4]^{2-}$), 505.2 ($[L - H]^-$), 554.3 ($[2\,L + SO_4]^{2-}$), 603.1 ($[L + HSO_4]^-$). Anal. Found: C, 46.90; H, 5.38; N, 22.78. Calcd. For $[Fe(DABP)_3][SO_4{\subset}L]\cdot 9H_2O$ ($C_{54}H_{78}FeN_{22}O_{16}S$): C, 47.04; H, 5.70; N, 22.34%. FT-IR (KBr, ν/cm^{-1}): 3338 m (br.), 3221 m (br.), 3050 m, 2813 w, 1667 s (br.) (C═O), 1601 s, 1575 s, 1550 s (br.), 1485 s, 1416 m, 1297 m, 1264 m, 1229 m, 1191 w, 1116 m (br.), 1066 m, 1028 w, 974 w, 880 w, 842 w, 802 w, 707 w, 612 w, 562 w, 542 w, 449 w, 406 w.

Competitive Experiment for Tetrahedral Anions in Solution. A methanol solution of L (1 equiv) was combined with an aqueous solution containing 1 equiv of $[Fe(DABP)_3]SO_4$, K_2CrO_4, and K_3PO_4, respectively, and the reaction mixture was used for ESI-MS test. Negative-ion mode ESI-MS: 301.5, $[L + SO_4]^{2-}$ or $[L + HPO_4]^{2-}$; 554.7, $[2\,L + SO_4]^{2-}$ or $[2\,L + HPO_4]^{2-}$; 603.7, $[L + HSO_4]^-$ or $[L + H_2PO_4]^-$; 564.7, $[2\,L + CrO_4]^{2-}$; 623.7 $[L + HCrO_4]^-$.

X-ray Crystallography. Diffraction data for the compounds **2** and **3** were collected on a Bruker SMART APEX II diffractometer at room temperature (293 K) with graphite-monochromated Mo Kα radiation (λ = 0.71073 Å). An empirical absorption correction using SADABS was applied for all data.[11] The structures were solved by direct methods using the SHELXS program.[11] All non-hydrogen atoms were refined anisotropically by full-matrix least-squares on F^2 by the use of the program SHELXL.[12] Hydrogen atoms bonded to carbon and nitrogen were included in idealized geometric positions with thermal parameters equivalent to 1.2 times those of the atom to which they were attached. Hydrogen atoms of the crystalline water molecules were not included.

Crystal data for **2**: $C_{54}H_{80}FeN_{22}O_{17}S$ (1397.31), red block, crystal system: trigonal, space group: $R\bar{3}c$, a = 13.812(1), b = 13.812(1), c = 121.731(1) Å, γ = 120°, V = 20112(3) Å^3, T = 293(2) K, Z = 12, D_c = 1.384 g cm^{-3}, F_{000} = 8832, μ = 0.34 mm^{-1}, 34970 refl. collected, 4625 unique (R_{int} = 0.125), 1269 observed [$I > 2\sigma(I)$]; final $R1$ = 0.086, $wR2$ = 0.238 [$I > 2\sigma(I)$]. CCDC 721311. It should be noted that compound **2** displays the typical graphite-type layered structure with a long *c*-axis (ca. 121 Å) and twelve layers in the unit cell (Supporting Information, Figure S3). We have repeated the structural measurement using crystals from different preparations, and the current structure is reproducible. The purity of the product was confirmed by powder X-ray diffraction (PXRD) studies and elemental analysis. Nevertheless, in one case another packing mode was obtained, with a shorter *c*-axis (compound **2′**, see Supporting Information).

Crystal data for **3**: $C_{54}H_{60}FeN_{16}O_{16}S$ (1289.19), red block, crystal system: trigonal, space group: $R\bar{3}c$, a = 13.9945(9), b = 13.9945(9), c = 116.519(16) Å, γ = 120°, V = 19763(3) Å^3, T = 293(2) K, Z = 12, D_c = 1.300 g cm^{-3}, F_{000} = 8136, μ = 0.335 mm^{-1}, 40415 refl. collected, 3783 unique (R_{int} = 0.068), 2297 observed [$I > 2\sigma(I)$]; final $R1$ = 0.080, $wR2$ = 0.24 [$I > 2\sigma(I)$].

Results and Discussion

The compound $[Fe(DABP)_3][LSO_4]\cdot 10H_2O$ (**2**) was obtained as red crystals by slow evaporation of a solution of $[Fe(DABP)_3]SO_4$ with equimolar ligand L in water−methanol (50:50 v/v). Slow diffusion of diethyl ether into a methanol solution containing a mixture of $[Fe(bipy)_3]SO_4$ and equimolar ligand L gave red crystals of **3**, $[Fe(bipy)_3][LSO_4]\cdot 9H_2O$. Compound **2** is soluble in methanol and DMSO, sparingly soluble in water and ethanol, while **3** is soluble in water, methanol, ethanol, and DMSO, and slightly soluble in acetonitrile.

The structure of compound **2** is built of the $[Fe(DABP)_3]^{2+}$ cations, $[SO_4{\subset}L]^{2-}$ anionic units, and two types of water clusters, that is, water tetramers and octamers. The ratio of L to SO_4^{2-} is 1:1, and each L includes a sulfate anion in its cleft via nine hydrogen bonding interactions (Figure 1). The urea NH groups of the three arms all point to the inside of the cavity, forming six N−H···O hydrogen bonds with the sulfate ion. There are also three additional C−H···O contacts around each SO_4^{2-} anion. One of the oxygen atoms (O2) sits at the C_3 axis and thus accepts three N−H···O bonds (N7···O2, 2.940(9) Å; ∠N7−H7B···O2, 166.3°), while each of the other three O atoms (which are related by C_3 symmetry) forms one N−H···O (N6···O3, 2.947(10) Å; ∠N6−H6A···O3, 154.2°) and one C−H···O (C11···O3, 3.056 Å; ∠C11−H11A···O3, 140.5°) hydrogen bond. This is remarkably different from the complete sulfate encapsulation by two L molecules in the $[M(H_2O)_6][SO_4{\subset}L_2]$ compounds, in which 11 N−H···O bonds were found between the 12 NH groups and the 4 O atoms of SO_4^{2-}.[7a]

The $[SO_4{\subset}L]^{2-}$ moieties and the $[Fe(DABP)_3]^{2+}$ cations in **2** align in the *ab* plane, forming a corrugated 2D layer (Figure 2).[13] Both of them are located at the C_3 axes and are linked to each other by N−H···O hydrogen bonds between the amino groups of DABP and the oxygen atoms of urea carbonyl groups (N2···O1, 2.967(8) Å; ∠N2−H2A···O1, 121.2°). Viewed down the *c* axis, three $[SO_4{\subset}L]^{2-}$ or $[Fe(DABP)_3]^{2+}$ units are arranged as a regular triangle (side length Fe−Fe or N−N: 13.8 Å). Each

(11) Sheldrick, G. M. *SADABS: Area-Detector Absorption Correction*; University of Göttingen: Göttingen, Germany, 1996.

(12) Sheldrick, G. M. *SHELXS-97, SHELXL-97, Programs for Crystal Structure Analysis*; University of Göttingen: Göttingen, Germany, 1997.

(13) (a) Fabelo, O.; Pasán, J.; Cañadillas-Delgado, L.; Delgado, F. S.; Labrador, A.; Lloret, F.; Julve, M.; Ruiz-Pérez, C. *CrystEngComm* **2008**, *10*, 1743–1746. (b) Ye, B.-H.; Ding, B.-B.; Weng, Y.-Q.; Chen, X.-M. *Inorg. Chem.* **2004**, *43*, 6866–6868.

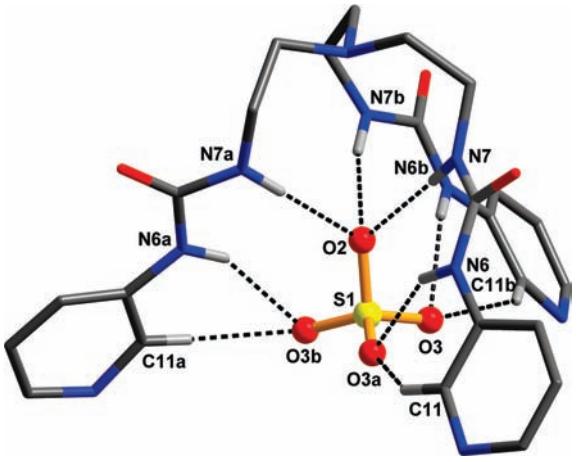

Figure 1. Sulfate ion inclusion in the $[SO_4 \subset L]^{2-}$ anionic unit in **2**. Non-interacting hydrogen atoms are omitted for clarity. Symmetry code: a, $-x+y, 1-x, z$; b, $1-y, 1+x-y, z$.

$[SO_4 \subset L]^{2-}$ is located at the center of a triangle formed by three $[Fe(DABP)_3]^{2+}$ complexes and accepts three N−H···O bonds. On the other hand, each $[Fe(DABP)_3]^{2+}$ cation sits at the center of a triangle formed by three $[SO_4 \subset L]^{2-}$ moieties. It is noticed that the hydrogen bonding interactions between the cation and anion in **2** are different from those in **1**. The first-sphere ligand DABP in **2** forms only N−H···O bonds through the amino group with the urea carbonyl group of the tris(pyridylurea) L, while each of the coordinated water molecules in **1** donates hydrogen bonds both to the carbonyl (O−H···O) and pyridyl groups (O−H···N) of L. The pyridyl nitrogen is involved in the hydrogen bonding with the crystalline water molecules in **2**.

There are two types of water clusters,[13a] namely, water tetramers and octamers, in the structure of **2**. The four oxygen atoms of the water tetramer form a parallelogram (O···O distances: 2.795 and 2.917 Å, and O−O−O angles: 62.0 and 118.0°, respectively; see Figure 3a), which links two inversion-related layers via two O−H···N hydrogen bonds with the pyridyl N atom of L (O5···N5, 2.739 Å). The distorted "water cube" (octamer), with eight short O···O edges (2.787−3.056 Å) and four longer (weaker) O···O contacts (3.667 Å, Figure 3b), accepts six N−H···O hydrogen bonds (N2···O6, 3.206(13) Å) from the amino groups of six $[Fe(DABP)_3]^{2+}$ cations (Figure 3c). Thus, the layers containing the $[SO_4 \subset L]^{2-}$ moieties and the $[Fe(DABP)_3]^{2+}$ cations are further linked by alternative water parallelograms and quasi-cubes and are packed along the *c* axis to form a 3D supramolecular structure (Figure 4a). Notably, the compound can partially lose the crystalline water molecules even at room temperature, as shown by the TGA (Supporting Information, Figure S2) and elemental analysis. It is known that the $[Fe(DABP)_3]^{2+}$ complexes are chiral. Within a layer, the $[Fe(DABP)_3]^{2+}$ units adopt the same Δ or Λ configuration. Two adjacent monolayers linked by the water tetramers are of opposite configurations, while two of the $(H_2O)_8$-related layers consist of $[Fe(DABP)_3]^{2+}$ units with the same configuration (Λ, Δ, Δ, Λ in Figure 4a, from top to bottom).

When $[Fe(bipy)_3]SO_4$ was used to react with the tris(pyridylurea) ligand L, an analogous compound, $[Fe(bipy)_3][SO_4 \subset L] \cdot 9H_2O$ (**3**), was isolated, which is essentially isomorphous with **2**. In compound **3**, the sulfate ion is also half-encapsulated in the cleft of one L molecule

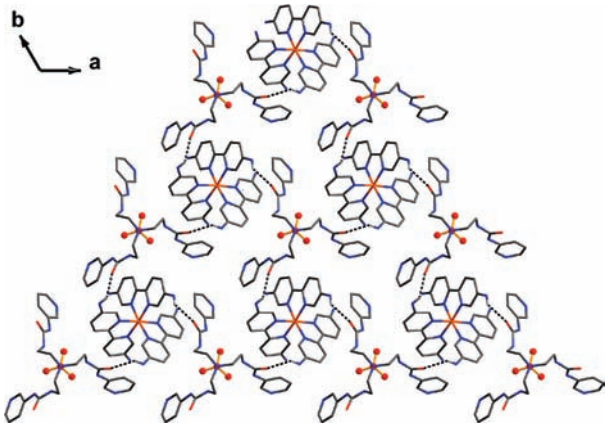

Figure 2. $[SO_4 \subset L]^{2-}$ anionic units and $[Fe(DABP)_3]^{2+}$ cations align in the *ab* plane, forming a 2D layer via N−H···O hydrogen bonding.

(Supporting Information, Figure S8). Although there is no hydrogen bonding between $[Fe(bipy)_3]^{2+}$ cations and $[SO_4 \subset L]^{2-}$ anionic units in **3** because of the absence of the hydrogen-bond donors (the amino groups), the arrangement of the two building blocks is almost identical to that in **2** (Supporting Information, Figure S9) with a layered structure (Figure 4b). The difference between **2** and **3** is that there are single water molecules (Supporting Information, Figure S8), water dimers and hexamers (Figure 3d, e, f) in **3** between the layers formed by $[Fe(bipy)_3]^{2+}$ cations and $[SO_4 \subset L]^{2-}$ anionic units. Each of the O3 atoms of sulfate ion (related by C_3 symmetry) accepts one O−H···O (O6···O3, 3.0 Å) hydrogen bond from a single water molecule. Each water dimer links two inversion-related layers via two O−H···N hydrogen bonds (O5···N5, 2.750 Å) with the pyridyl N atom of two L molecules (Figure 3d). The cyclic centrosymmetric water hexamer[13b] adopts the chair conformation (O···O distances: 2.745 Å, O−O−O angles: 100.0°; Figure 3e) and donates six O−H···O hydrogen bonds (O4···O1, 2.758 Å) to the urea groups of L (Figure 3f). As in the case of compound **2**, the $[Fe(DABP)_3]^{2+}$ complexes in the two adjacent monolayers linked by the water dimers are of the same configuration, while in the adjacent layers linked by the water hexamers, they adopt the opposite configurations (Λ, Λ, Δ, Δ, in Figure 4b, from top to bottom).

^{1}H NMR spectrum of compound **2** shows significant downfield chemical shifts (Δδ 1.93 and 1.48 ppm) of the two urea NH protons relative to L in DMSO-d_6 (Figure 5). These changes are considerably larger than those for the previously reported $[Zn(H_2O)_6][SO_4 \subset L_2]$ compound (Δδ 1.01 and 0.74 ppm, corresponding to a binding constant (log *K*) of 6.42 in DMSO),[7a] which may indicate stronger binding in compound **2**. Unfortunately, NMR titration of L with $[Fe(DABP)_3]SO_4$ was not possible because of the limited solubility of $[Fe(DABP)_3]SO_4$ in aprotic solvents, while the NH signals could not be observed in protic solvents. On the other hand, the compound **3** decomposes in DMSO-d_6 as confirmed by its ^{1}H NMR spectrum (Supporting Information, Figure S12) which prohibits further studies by NMR spectroscopy.

A comparison with our previous report of the $[M(H_2O)_6][SO_4 \subset L_2]$ compound (**1**) shows that the cationic part appears to have a great effect on the solid-state structure. In the case of compound **1**, the $[M(H_2O)_6]^{2+}$ ions led to complete encapsulation of sulfate by two tris(pyridylurea)

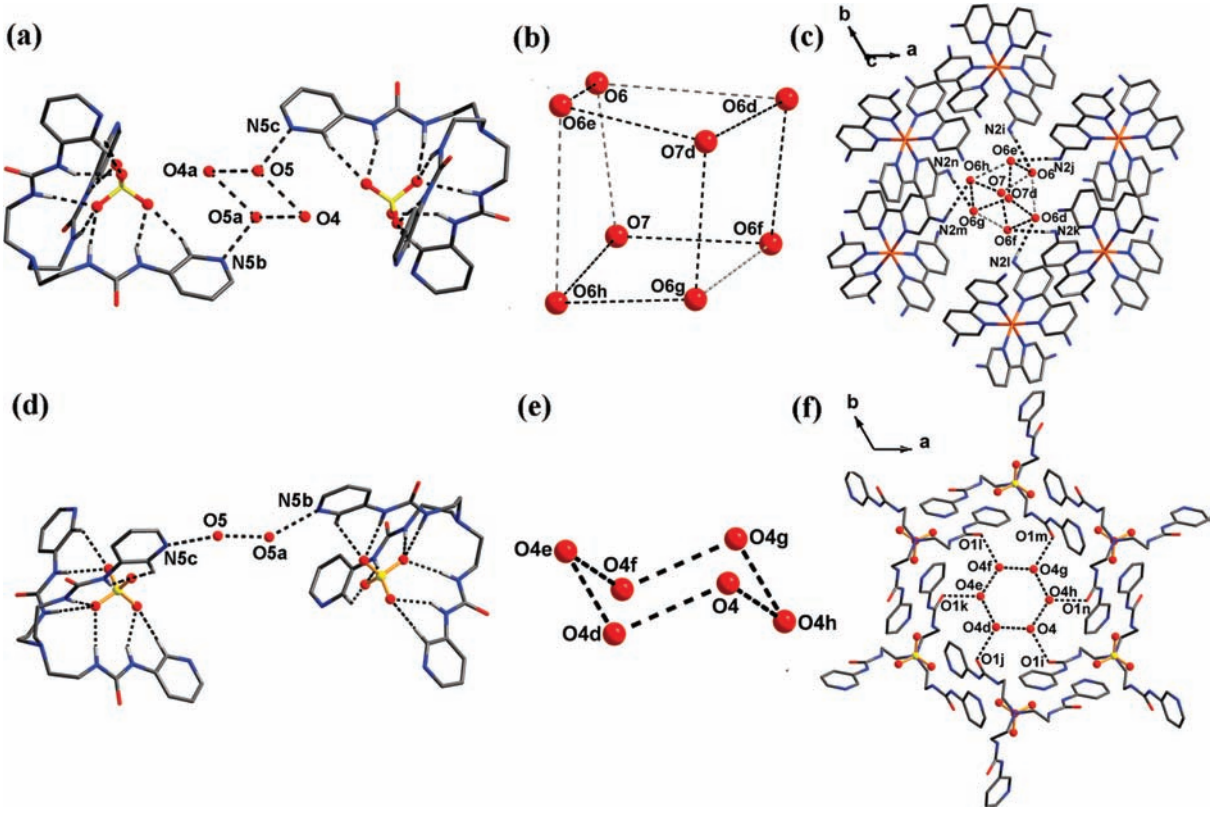

Figure 3. (a) Water parallelogram that links two adjacent, inversion-related layers via hydrogen bonding in **2**. (b) "Water cube" associated by hydrogen bonding. (c) N−H···O hydrogen bonds between one "water cube" and six $[Fe(DABP)_3]^{2+}$ cations viewed along the *c* axis. (d) Water dimer that links two adjacent layers in **3**. (e) The cyclic water hexamer with the chair conformation. (f) Hydrogen bonds between one water hexamer and six L molecules viewed along the *c* axis. Symmetry codes for the operations labeled in the structures, see the Supporting Information.

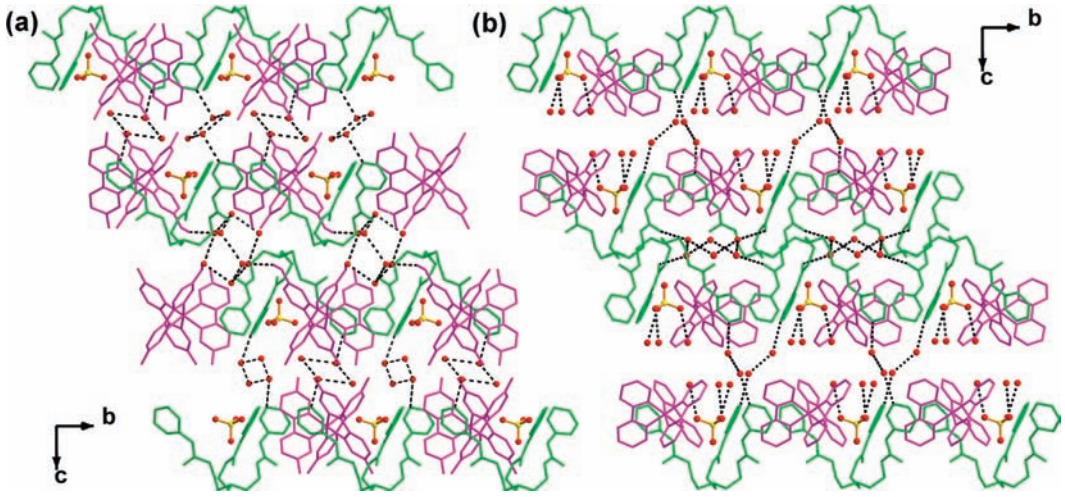

Figure 4. Layered structure (a) with water parallelograms and "water cubes" in **2**; and (b) with single water, water dimers and hexamers in **3**, located between the layers.

ligands,[7a] whereas the use of the larger first-sphere complex $[Fe(DABP)_3]^{2+}$ or $[Fe(bipy)_3]^{2+}$ resulted in half-encapsulation of SO_4^{2-} by only one ligand molecule in this work. However, the solution behavior showed some difference from the solid-state structure. In the negative-ion mode mass spectra of **2** and **3** (Figure 6c and Supporting Information, Figure S10b), both the 1:1 (301.0 in **2** and **3**, $[L + SO_4]^{2-}$; and 603.1 in **2** and 603.3 in **3**, respectively, $[L + HSO_4]^-$) and 1:2 (554.3 in **2** and **3**, $[2\ L + SO_4]^{2-}$) anion complexes are found, which is similar to the case of **1**. The

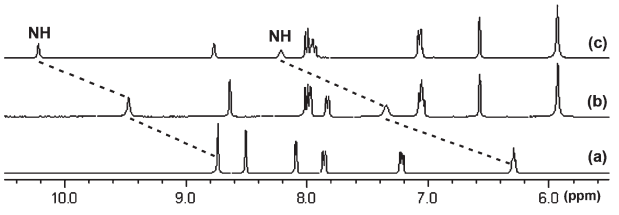

Figure 5. Downfield shifts of the urea NH groups upon addition of $[Fe(DABP)_3]SO_4$ to the solution of L in DMSO-d_6. (a) L; (b) L + 0.5 equiv of $[Fe(DABP)_3]SO_4$; (c) The compound $[Fe(DABP)_3][SO_4 \subset L] \cdot 10H_2O$.

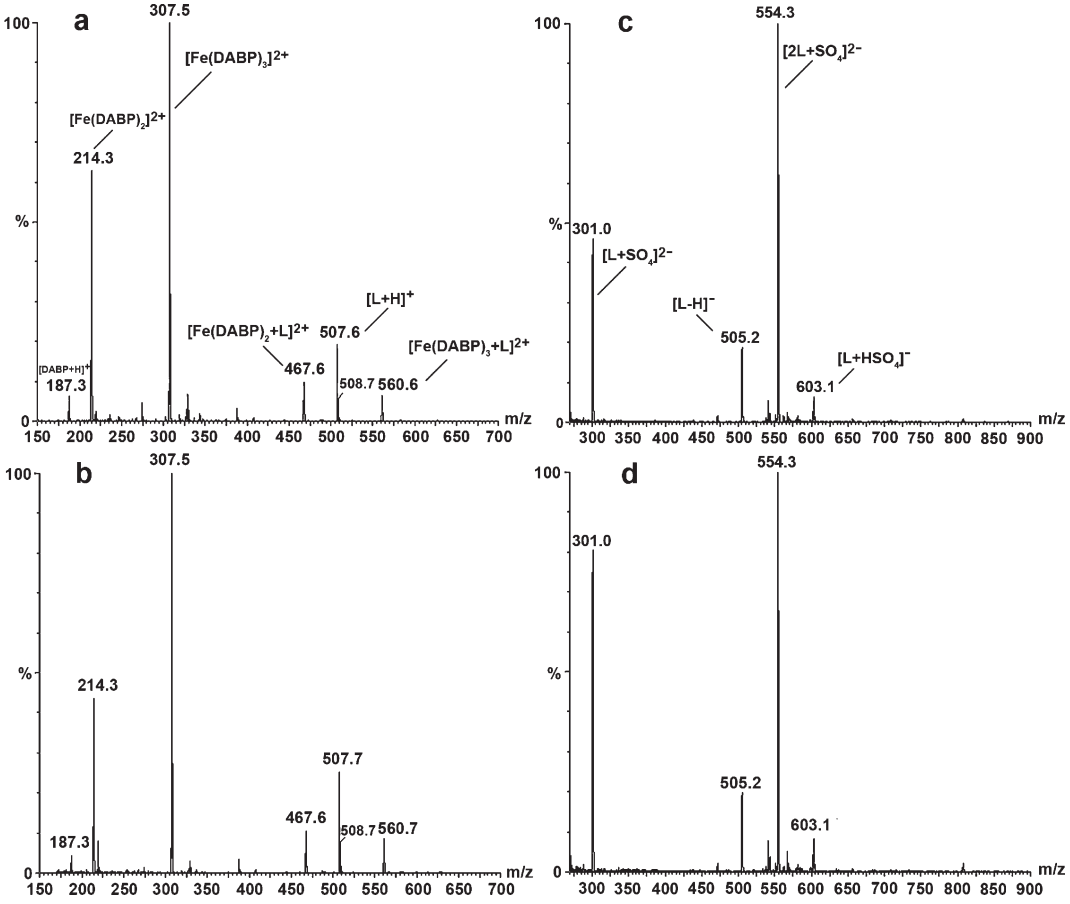

Figure 6. ESI-MS spectra of compound **2** (a, positive-ion mode; c, negative-ion mode) and the product **2a** obtained in the presence of SO_4^{2-}, OAc^-, NO_3^- and ClO_4^- anion mixture (b, positive-ion mode; d, negative-ion mode).

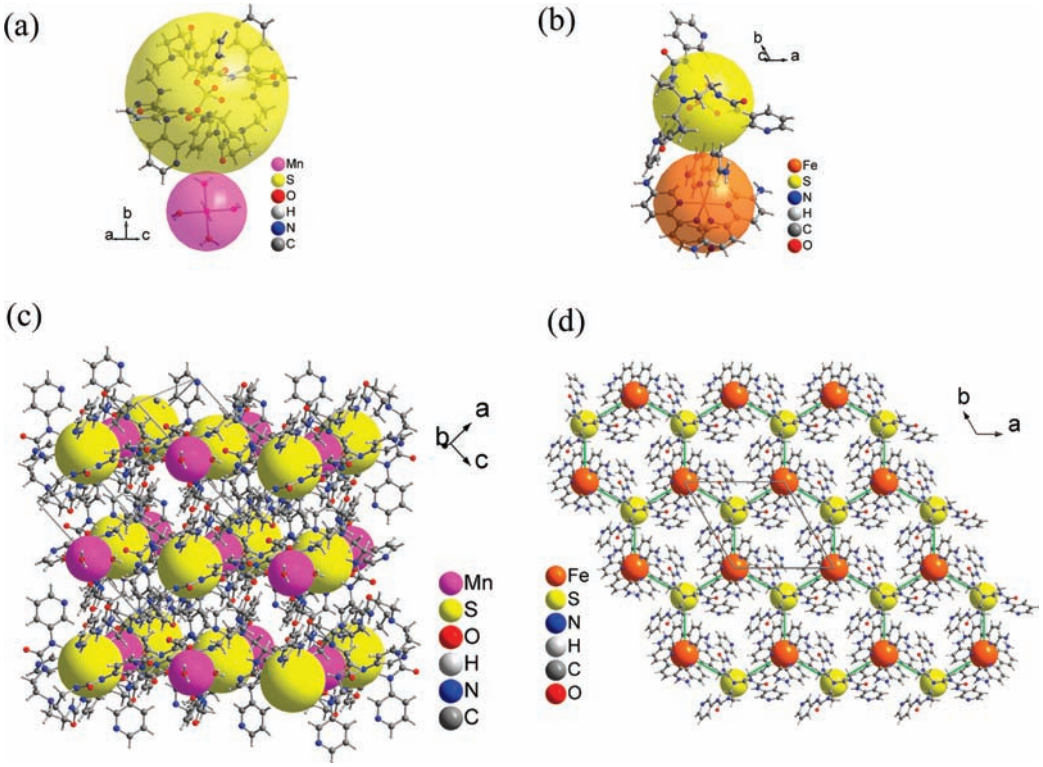

Figure 7. Solid-state correlation of **1** and **2**. (a) Approximated cation and anion vdW radii in **1** as space-filling pink and yellow spheres; (b) approximated cation and anion vdW radii in **2** as orange and yellow spheres, respectively; (c) NaCl-type structure of **1**; (d) Hexagonal BN-structure of **2** with green connecting lines as visual aids, both packing diagrams have the radii of the space-filling spheres reduced for better visibility.

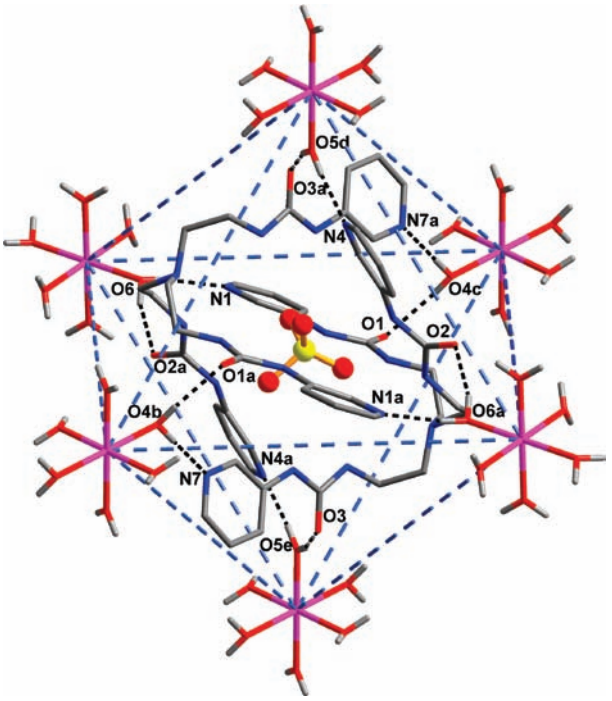

Figure 8. Octahedral anion−cation packing in compound **1a** (ref 7a) directed by hydrogen bonding interactions between a coordinated water molecule and the pyridyl or the carbonyl group in L. Hydrogen bond parameters (Å, deg): O4b···N7, 2.728(2), 180(2); O5e···N4a, 2.727(2), 175(2); O6a···N1a, 2.789(2), 170(2); O4c···O1, 2.835(2), 158(2); O5d···O3a, 2.7151(16), 168(2); O6···O2a, 2.7599(19), 164(2). Symmetry code: a, $-x$, $1-y$, $1-z$; b, $-1/2-x$, $1/2+y$, $3/2-z$; c, $1/2+x$, $1/2-y$, $-1/2+z$; d, $-1/2+x$, $1/2-y$, $-1/2+z$; e, $1/2-x$, $1/2+y$, $3/2-z$.

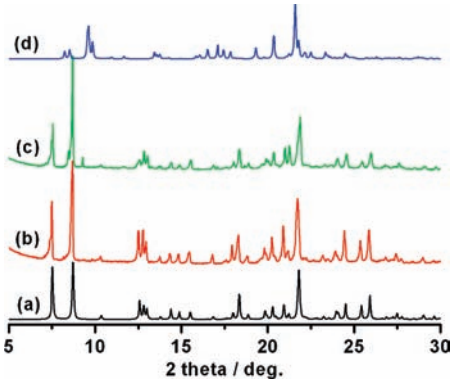

Figure 9. PXRD patterns. (a) Simulated from the single-crystal X-ray data of **2**; (b) experimental pattern of **2**; (c) experimental pattern from the crystals crystallized in the presence of SO_4^{2-}, OAc^-, NO_3^-, and ClO_4^-; and (d) simulated from the 1:2 complex $[Mn(H_2O)_6][SO_4{\subset}L_2]$ (**1a**) (ref 7a).

positive-ion mode ESI-MS spectrum of **2** is dominated by a peak at m/z 307.5 (100%) for the $[Fe(DABP)_3]^{2+}$ cation with a minor component at m/z 560.6 (ca. 5%) for the divalent $[Fe(DABP)_3(L)]^{2+}$ fragment (Figure 6a), which agrees well with the calculated value of 560.2. Although a peak at m/z 262.4 (100%) for the $[Fe(bipy)_3]^{2+}$ cation exists in the ESI-MS of **3**, no $[Fe(bipy)_3(L)]^{2+}$ fragment is observed (Supporting Information, Figure S10b). These data are in agreement with the fact that the $[Fe(DABP)_3]^{2+}$ cation and L are linked by hydrogen bonds in **2** but there is no hydrogen bonding interaction between $[Fe(bipy)_3]^{2+}$ and L in **3**.

To gain deeper insight into the solid-state structures of **1**, **2**, and **3**, and to understand the reason for the occurrence of the

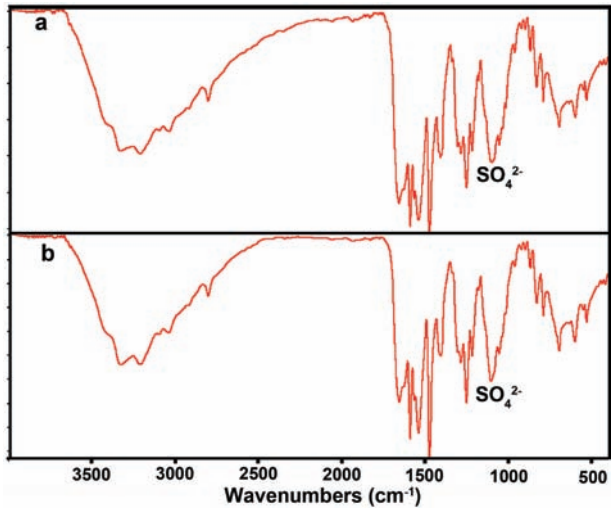

Figure 10. FT-IR spectra of the competitive crystallization experiments. (a) Crystals obtained from SO_4^{2-} alone. (b) Crystals obtained in the presence of SO_4^{2-}, OAc^-, NO_3^-, and ClO_4^- anion mixture.

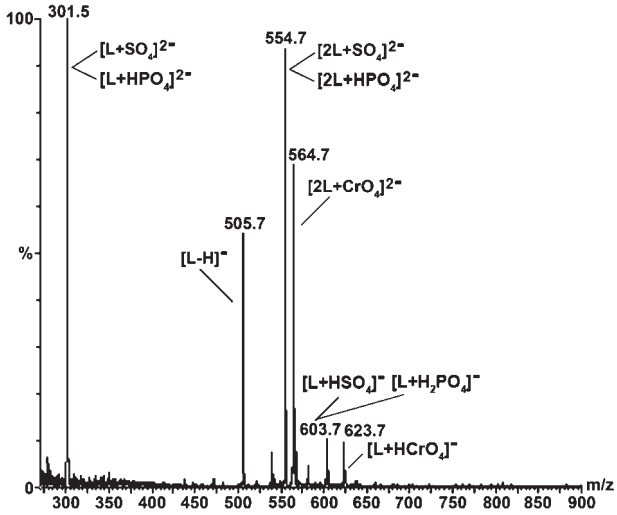

Figure 11. Negative-ion mode ESI-MS spectrum of the competition reaction of L, $[Fe(DABP)_3]SO_4$, K_2CrO_4, and K_3PO_4.

1:1 $[SO_4{\subset}L]$ or 1:2 $[SO_4{\subset}L_2]$ capsule, a correlation of the secondary coordination sphere and the crystal packing of the overall structure has been studied. The $[Mn(H_2O)_6][SO_4{\subset}L_2]$ compound (**1a**) shows a NaCl-type structure with $[Mn(H_2O)_6]^{2+}$ as the cation (estimated average van der Waals radius ca. 3.2 Å) and the capsule $[SO_4{\subset}L_2]^{2-}$ as the anion (est. av. vdW radius ca. 6.5 Å) (Figure 7a,c).[7a] For the half-encapsulating compounds **2** and **3**, the space-filling radii were estimated to be ~4 Å for both the $[Fe(DABP)_3]^{2+}$ or $[Fe(bipy)_3]^{2+}$ cation and the $[SO_4{\subset}L]^{2-}$ anion, when taking into account the now quite aspherical shape of the anion. As described above, these two compounds are 2D layers showing the graphite structure with each hexagon consisting of alternating cations and anions, like in hexagonal BN (Figure 7b,d).

In the three supramolecular systems, the pyridyl functions of the tris(pyridylurea) ligand L are not involved in the direct coordination with the metal ions, and thus serve as very good hydrogen-bond acceptors. In **1a** the $[M(H_2O)_6]^{2+}$ cation can satisfy this hydrogen-acceptor property through $O_w{-}H\cdots N_{py}$ bonding (Figure 8). The octahedral $[M(H_2O)_6]^{2+}$ cation may

actually help in the formation of an octahedral cation−anion coordination in the NaCl-type structure. Moreover, the $[SO_4\subset L_2]^{2-}$ anion has six pyridyl acceptors, which is certainly advantageous for the octahedral packing.

In contrast, in compounds **2** and **3** the cation ($[Fe(DABP)_3]^{2+}$ or $[Fe(bipy)_3]^{2+}$) has only weaker ($-NH_2$ of DABP) or no (bipy) hydrogen donor sites and can not form hydrogen bonds with the pyridyl nitrogen (the amino groups in **2** form $N-H\cdots O_{C=O}$ contacts with the urea carbonyl groups of L). Therefore, crystal water has to come in to satisfy the hydrogen-accepting demands of L (Figure 3a,d). If there is still a $[SO_4\subset L_2]^{2-}$ anion, it would be surrounded by crystal water molecules which could lower the Coulomb-attraction (and consequently the lattice energy) between the cation and anion, hence preventing the efficient crystallization of such a species. On the other hand, the non-spherical and only partly water-surrounded $[SO_4\subset L]^{2-}$ anion allows for a closer approach of the $[Fe(DABP)_3]^{2+}$ or $[Fe(bipy)_3]^{2+}$ cation than the $[SO_4\subset L_2]^{2-}$ anion. Furthermore, the hydration of the $[SO_4\subset L]^{2-}$ anion leads to an anisotropic Coulomb attraction, as the cation−anion separation between the layers is at least 3 Å longer (>11.2 Å) than within the layers (~8 Å) because of the presence of the interlayer water clusters (while in **1a** the anion capsule is not hydrated and the Coulomb attraction is equal in all three directions). Thus, in **2** and **3** the cation−anion Coulomb attraction is confined to a two-dimensional plane, which corresponds to the layered structure. Since the cation and anion in **2** and **3** have about the same size, a hexagonal BN (or graphite) lattice is formed. Therefore, the encapsulation of sulfate by one versus two L molecules may indeed be traced to the hydrogen bonding properties of the secondary coordination sphere which effectively affect the cation−anion Coulomb attraction in the solid-state packing. It should be noted that the full- or half-encapsulation of sulfate is observed only in the solid state, while in solution all the three compounds show both the 1:1 and 1:2 sulfate-to-ligand ratios as mentioned above.

The sulfate selectivity against other anions was studied by a competition crystallization experiment, which resulted in a compound (**2a**) identical to **2** as confirmed by XRD (Figure 9) and elemental analysis. The FT-IR spectra (Figure 10) of compounds **2** and **2a** display similar characteristic peaks for sulfate anion at 1111 and 1116 cm^{-1}, respectively, and no detectable amounts of NO_3^-, OAc^-, or ClO_4^- were found in the crystallized material. The ESI-MS spectra of the competition product **2a** (Figure 6) match well with those of **2**, which further support the sulfate separation by selective crystallization of the sulfate complex **2**. Furthermore, comparative anion recognition for isoelectronic tetrahedral anions SO_4^{2-}, CrO_4^{2-}, and PO_4^{3-} was examined by ESI-MS spectrometry. For the strongly basic PO_4^{3-} the protolytic equilibrium yields HPO_4^{2-} as the most abundant species between pH 7−11 in aqueous solution, followed by $H_2PO_4^-$ around and below pH 7.[14] Since SO_4^{2-} and HPO_4^{2-} have the same charge and same rounded mass of 96, an isotope abundance does not allow for a distinction of them, as phosphorus is an isotope-pure element and the abundance of ^{34}S as the only other significant sulfur isotope (besides ^{32}S) is only 4%. Thus, the mixture of L, $[Fe(DABP)_3]SO_4$, K_2CrO_4, and K_3PO_4 showed negative ions ([L·anion] and [L_2·anion]) at 301.5 for $[L + SO_4]^{2-}$ or $[L + HPO_4]^{2-}$; 554.7 for $[2\ L + SO_4]^{2-}$ or $[2\ L + HPO_4]^{2-}$; 603.7 for $[L + HSO_4]^-$ or $[L + H_2PO_4]^-$, and 564.7 for $[2\ L + CrO_4]^{2-}$ and 623.7 for $[L + HCrO_4]^-$, respectively (see Figure 11). While the binding of SO_4^{2-} and PO_4^{3-}/HPO_4^{2-} could only be clearly discerned with a high-resolution MS experiment, the binding of CrO_4^{2-} is competitive to SO_4^{2-} and PO_4^{3-}/HPO_4^{2-}. The competition between SO_4^{2-} and PO_4^{3-}/HPO_4^{2-} will be addressed in future work.

Conclusions

In summary, we obtained two supramolecular architectures, $[Fe(DABP)_3][SO_4\subset L]\cdot 10H_2O$ (**2**) and $[Fe(bipy)_3][SO_4\subset L]\cdot 9H_2O$ (**3**), via the self-assembly of $[Fe(DABP)_3]SO_4$ or $[Fe(bipy)_3]SO_4$ with a tris(3-pyridylurea) ligand (L). The two compounds show a similar layered structure, in which each ligand molecule includes a sulfate anion in its cleft via multiple hydrogen bonds. Alternative water parallelograms and quasi "water cubes" link the 2D layers formed by $[SO_4\subset L]^{2-}$ anionic units and $[Fe(DABP)_3]^{2+}$ cations into a 3D network in compound **2**, while in **3** single water molecules, water dimers and hexamers are found between the layers. FT-IR, PXRD, and elemental analysis reveal that SO_4^{2-} can be selectively crystallized from an aqueous solution containing other oxoanions, such as NO_3^-, OAc^-, and ClO_4^-, as competing anions. The encapsulation of sulfate by a single ligand molecule rather than two receptors is rationalized by the better solid-state packing mode of the complex cations $[Fe(DABP)_3]^{2+}$ and $[Fe(bipy)_3]^{2+}$ without sufficient secondary hydrogen-bond donors and half-encapsulated anions $[SO_4\subset L]^{2-}$.

Acknowledgment. This work was supported by the National Natural Science Foundation of China (Grant 20872149) and the "Bairen Jihua" project of the Chinese Academy of Sciences.

Supporting Information Available: The crystallographic data for **2**, **2′**, and **3** in CIF format, and the characterizations for **2** and **3**. This material is available free of charge via the Internet at http://pubs.acs.org.

(14) Craven, E.; Abu-Shandi, K.; Janiak, C. *Z. Anorg. Allg. Chem.* **2003**, *629*, 195–201.